Journal of Organometallic Chemistry, 339 (1988) 139–149
Elsevier Sequoia S.A., Lausanne – Printed in The Netherlands

Electronic structure of $Os_3(CO)_8(C_2Ph_2)_2$: deformation of a trimetal framework by acetylene ligands

Catherine E. Housecroft* and Steven M. Owen

University Chemical Laboratory, Lensfield Road, Cambridge, CB2 1EW (Great Britain)

(Received July 10th, 1987)

Abstract

The electronic structure of $Os_3(CO)_8(C_2Ph_2)_2$ is discussed. Each acetylene ligand is bonded to the triosmium framework via a μ_3-η^2-mode, the C–C bond vectors being parallel to a common Os–Os edge. Thus, each alkyne can be viewed as forming a π-bond to one osmium atom, and two σ-bonds to the other two osmium atoms. This simple bonding description is confirmed by the results of a Fenske–Hall molecular orbital analysis. Compared to $Os_3(CO)_{12}$, $Os_3(CO)_8(C_2Ph_2)_2$ exhibits a significantly deformed metal carbonyl framework. The first deformation is a noticeable shortening of two of the metal–metal edges. This feature is shown to be due to a combination of direct metal–metal bonding and indirect metal–metal interaction via the acetylene ligands. The second framework deformation is a change in carbonyl orientation along the series $Os_3(CO)_{12-2x}(C_2Ph_2)_x$ ($x = 0, 1, 2$). This is shown to be essential for maximum metal–ligand interaction.

There have been several theoretical studies on the interactions of alkyne ligands with transition metal or borane frameworks [1–5]. Much interest has been shown in the weakening of the carbon–carbon bond within the acetylene as it coordinates to a metal framework. Previous work has focused attention on the so-called "parallel" and "perpendicular" modes of acetylenic coordination in compounds containing an M_3C_2 core [2,3,5]. The bis-acetylenic trimetal clusters, $Fe_3(CO)_8(C_2Ph_2)_2$ [6] and $Os_3(CO)_8(C_2Ph_2)_2$ [7] provide interesting examples of an $M_3(C_2)_2$ core in which the two alkynes remain unassociated with each other and reside on opposite sides of the metal triangle in symmetry related "parallel" positions. $Ru_3(CO)_8(C_2Ph_2)_2$ has been synthesized but its crystal structure has not been determined; however, X-ray powder diffraction studies suggest that the structure of the ruthenium cluster is analogous to those of the osmium and iron derivatives [8]. In the case of osmium, a progressive series $Os_3(CO)_{12-2x}(C_2Ph_2)_x$ ($x = 0, 1, 2$) is observed; as the first and then the second alkyne ligand binds, the metal framework is progressively deformed. One significant deformation is the shortening of two of the three Os–Os bonds.

0022-328X/88/$03.50

Granozzi et al. have suggested that, in the case of the related compound $Fe_3(CO)_9(C_2H_2)$, contraction of the metal triangle is required in order to accommodate the small alkyne ligand [3]. We illustrate below that the contraction noted in $Os_3(CO)_8(C_2Ph_2)_2$ is probably due to a combination of direct metal–metal and indirect metal–metal (i.e. via the ligand) bonding. A second framework deformation, observed as one moves along the series $Os_3(CO)_{12-2x}(C_2Ph_2)_x$ from $x = 0$ to 2, is a change in the carbonyl ligand orientations. We show that as a pair of carbonyls (each carbonyl being a two-electron donor) is replaced by an acetylene ligand (a four-electron donor), reorientation of the remaining carbonyl ligands takes place so as to maximize metal to acetylene bonding.

Experimental

Fenske–Hall [9] calculations were carried out by using $Ru_3(CO)_{12}$, and $Ru_3(CO)_8(C_2H_2)_2$ to model $Os_3(CO)_{12}$ and $Os_3(CO)_8(C_2Ph_2)_2$ respectively, since basis functions for osmium are not available. The structure of $Ru_3(CO)_8(C_2H_2)_2$ was idealized to C_{2v} symmetry. All C–O bonds were set at 1.13 Å and Ru–CO bonds at 1.92 Å. In $Ru_3(CO)_{12}$, Ru–Ru = 2.854 Å. Atomic numbering for $Ru_3(CO)_8(C_2H_2)_2$ is shown in Scheme 1; Ru(1)–Ru(2) = Ru(2)–Ru(3) = 2.70 Å, Ru(1)–Ru(3) 2.75, Ru(1)–C(4) = Ru(3)–C(5) = 2.19, Ru(2)–C(4) = R(2)–C(5) = 2.14, C(4)–C(5) 1.42, C–H 1.09 Å. The angle C(4)C(5)H is 127°. Atom pairs C(4) and C(4′), and C(5) and C(5′) are related by symmetry. For the calculations which compared carbonyl orientations in $Ru_3(CO)_8(C_2H_2)_2$ and $Ru_3(CO)_{12}$, the C–Ru–C bond angles were as shown in Table 1; the structures considered are shown in Fig. 6.

The Fenske–Hall calculations employed single-ζ Slater functions for the 1s and 2s functions of C and O. The exponents were obtained by curve fitting the double-ζ functions of Clementi [10] while maintaining orthogonal functions; the double-ζ

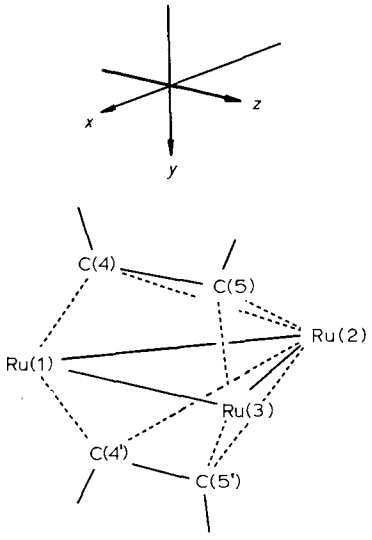

Scheme 1.

Table 1

C(carbonyl)–M–C(carbonyl) bond angles (°)

	$Os_3(CO)_8(C_2Ph_2)_2$ or $Ru_3(CO)_8(C_2H_2)_2$	$Os_3(CO)_{12}$ or $Ru_3(CO)_{12}$	III	I	II
C(12)–M(1)–C(13)	92.9	90.1	90.7	–	–
C(12)–M(1)–C(11)	97.4	179.2	98.7	–	180
C(11)–M(1)–C(13)	94.8	90.3	98.7	89.3	–
C(13)–M(1)–C(14)	–	102.8	–	104.5	–
C(11)–M(1)–C(14)	–	90.7	–	90.1	90.0
C(12)–M(1)–C(14)	–	89.8	–	–	90.0

functions were used directly for the $2p$ orbitals. An exponent of 1.16 was used for hydrogen. The Ru functions were augmented by $5s$ and $5p$ functions with exponents of 2.20 [11].

Results and discussion

Metal–acetylene bonding in $Ru_3(CO)_8(C_2H_2)_2$

The bonding in $Ru_3(CO)_8(C_2H_2)_2$ is considered in terms of the interactions of the two acetylene ligands with a triruthenium framework (Fig. 1). The orbitals of each acetylene unit which are involved in binding the ligands to the metal fragment are illustrated in Fig. 2 and can be regarded as having π-symmetry, either π_x, $\pi_x^\star$, π_y or $\pi_y^\star$ according to the axis system shown in Scheme 1. Lower lying filled σ-orbitals (carbon–carbon and carbon–hydrogen bonding) remain localised on the C_2H_2 fragments after ligation to the metal framework, and are therefore not considered further. Of the filled orbitals of the $Ru_3(CO)_8$ fragment, only four (MOs 43, 44, 50 and 52) are significantly involved in bonding to the acetylene ligands. In addition, five empty metal framework MOs (53–57) are involved. Representative orbitals are illustrated in Fig. 3.

The correlation diagram in Fig. 4 shows the orbital interactions between the $Ru_3(CO)_8$ fragment and the two C_2H_2 ligands. For simplicity, only those correlations which produce MOs in $Ru_3(CO)_8(C_2H_2)_2$ having both metal and ligand

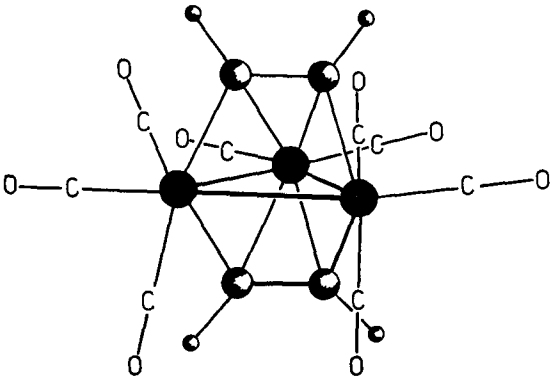

Fig. 1. Structure of the model compound $Ru_3(CO)_8(C_2H_2)_2$.

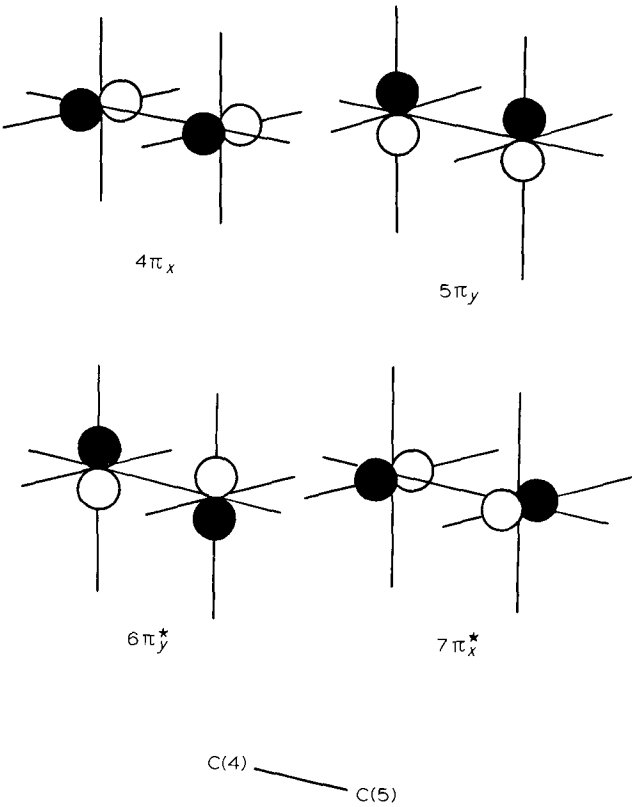

Fig. 2. Schematic representations of the fragment molecular orbitals of the C_2H_2 ligand.

character are presented. Note that the molecular symmetry of $Ru_3(CO)_8(C_2H_2)_2$ requires that both acetylene ligands interact in an equivalent manner with the triruthenium framework. Immediately it is apparent that the interactions can be separated into metal–carbon σ-interactions and metal–acetylene π-interactions. For example, MO 52 of the $Ru_3(CO)_8$ fragment is ideally suited to interact with MO 6 of the acetylene, leading to a donor–acceptor interaction which bonds the carbon atoms to Ru(1) and Ru(3) via σ-bonds while, at the same time, bonding the carbon–carbon multiple bond to Ru(2). Similarly, MO 55 of the trimetal fragment interacts with MO 5 of the acetylenes via both σ- and π-bonding modes (Fig. 5).

Table 2 lists Mulliken populations of the fragment orbitals both in the free fragments and in the complex $Ru_3(CO)_8(C_2H_2)_2$. The changes in the Mulliken populations of the acetylene ligand orbitals confirm the donor–acceptor interaction that one expects for a conventional metal–ligand Dewar–Chatt–Duncanson model interaction. Acetylene MOs 4 and 5 lose 0.44 and 0.45 electrons respectively, while MOs 6 and 7 gain 1.00 and 0.3 electrons respectively. Note that the fact that there are two alkyne ligands rather than one increases the number of orbital interactions. For example, an in-phase combination of the π_x orbitals (MO 5) will produce a bonding interaction with MO 55 of the $Ru_3(CO)_8$ fragment (Fig. 6) whereas an out-of-phase combination will interact with MOs 43 and 53. This produces a more complex bonding situation than is found when one acetylene ligand bonds to the

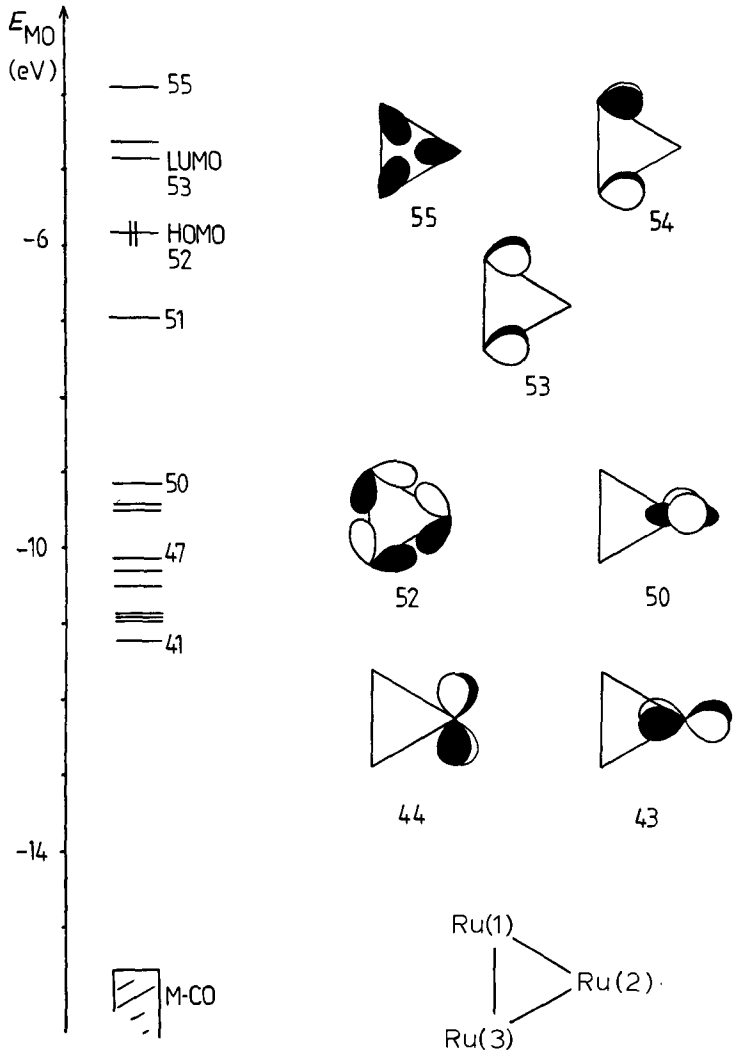

Fig. 3. Schematic representations of the molecular orbitals of the $Ru_3(CO)_8$ fragment.

same metal framework. However, it is important to remember that despite the metal–ligand bonding being interpreted as simple σ-donation and π-back-donation, a valence bond picture should not be envisaged. Fenske et al. [12] have emphasised that a molecular orbital treatment allows orbital interactions between two filled or between two empty fragment molecular orbitals. An analysis of the bonding in $Ru_3(CO)_8(C_2H_2)_2$ illustrates this fact since, for a multimetal system as opposed to a mononuclear metal-π-hydrocarbon complex, the range of symmetry allowed interactions between fragment (viz. metal and ligand) orbitals of appropriate energies extends beyond simple $\sigma_{ligand} \rightarrow \sigma_{metal}$ donation and $\pi_{metal} \rightarrow \pi^{\star}_{ligand}$ back-donation.

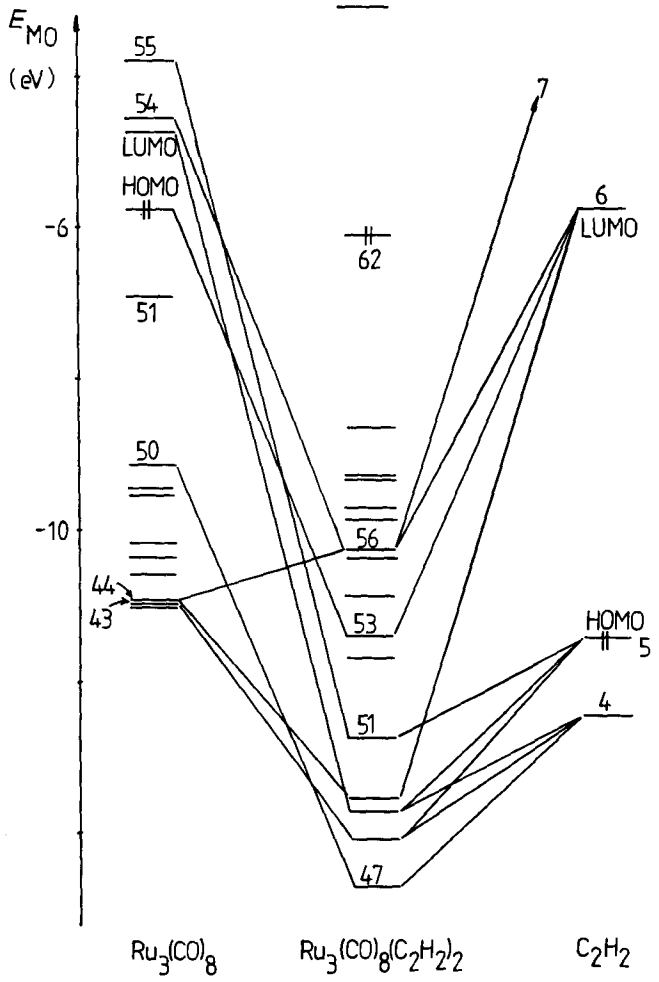

Fig. 4. Correlation of the molecular orbitals of the fragments $Ru_3(CO)_8$ and two C_2H_2 ligands in $Ru_3(CO)_8(C_2H_2)_2$.

Table 2

Mulliken populations of fragment orbitals before and after formation of $Ru_3(CO)_8(C_2H_2)_2$

$Ru_3(CO)_8$			C_2H_2		
MO	Orbital population in free $Ru_3(CO)_8$	Orbital population in complexed $Ru_3(CO)_8$	MO	Orbital population in free C_2H_2	Orbital population in complexed C_2H_2
48	2.00	1.78	4	2.00	1.56
49	2.00	1.54	5	2.00	1.55
50	2.00	1.93	6	0.00	1.00
51	2.00	0.90	7	0.00	0.30
52	2.00	0.86			
53	0.00	0.69			
54	0.00	1.04			
55	0.00	0.33			
56	0.00	0.10			
57	0.00	0.30			

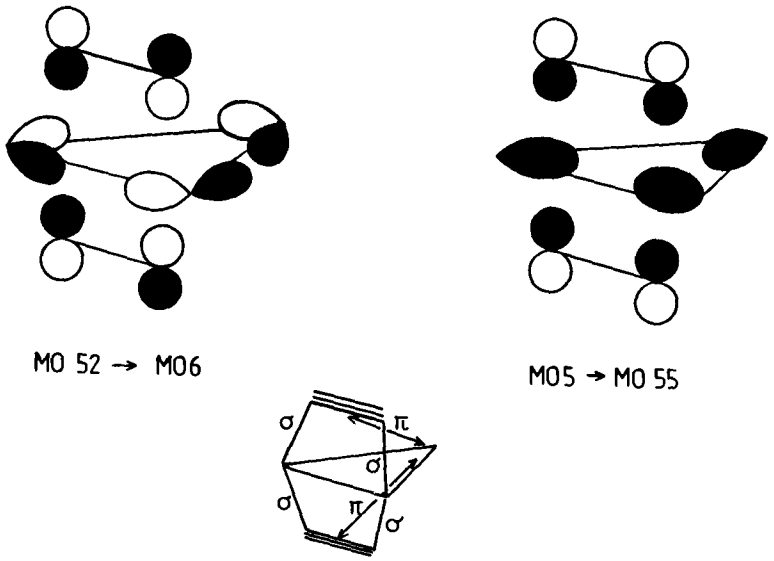

Fig. 5. Representative fragment molecular orbital interactions illustrating the Ru(1) and Ru(3)–acetylene σ-interactions and Ru(2)–acetylene π-interactions.

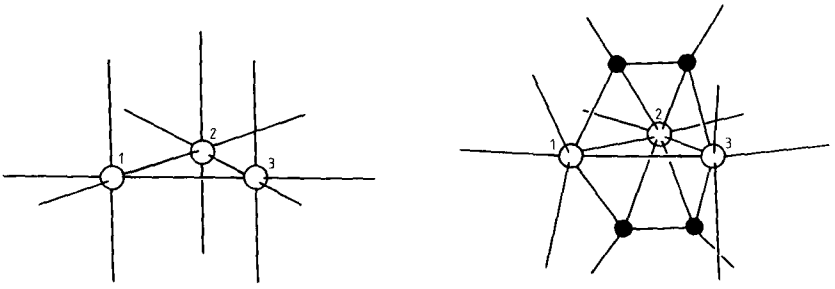

Fig. 6. Comparison of the carbonyl ligand orientations in $M_3(CO)_{12}$ and $M_3(CO)_8(C_2R_2)_2$ (M = Ru, Os; R = H, Ph).

Metal–metal bonding in $Ru_3(CO)_8(C_2H_2)_2$

Table 3 compares metal–metal Mulliken overlap populations in the $Ru_3(CO)_8$ fragment before and after interaction with the C_2H_2 units. (The geometry of the

Table 3

Metal—metal Mulliken overlap populations

Bond	Fragment		
	$Ru_3(CO)_8$	$Ru_3(CO)_8(C_2H_2)_2$	$Ru_3(CO)_{12}$
Ru(1)–Ru(2) Ru(2)–Ru(3)	+0.106	+0.073	+0.107
Ru(1)–Ru(3)	+0.110	+0.125	+0.107

metal triangle is kept constant and is that found in $Ru_3(CO)_8(C_2H_2)_2$.) There is a significant decrease in the Mulliken overlap population for Ru(1)–Ru(2) and Ru(2)–Ru(3), while the overlap population for Ru(1)–Ru(3) increases. The values for metal–metal overlap populations may seem to be small [12], but when compared to those in $Ru_3(CO)_{12}$, in which direct metal–metal bonding must be present, they appear to be quite reasonable. The main cause of the changes in metal–metal overlap populations in the ruthenium fragment is a loss of electron density from the HOMO (MO 52) of the $Ru_3(CO)_8$ fragment as it interacts with the acetylenes. The change from 2 electrons to 0.9 electrons in MO 52 is clearly significant. Examination of Fig. 3 shows how depopulation of MO 52 will influence metal–metal bonding; Ru(1)–Ru(2) and Ru(2)–Ru(3) will become weaker (less bonding) while Ru(1)–Ru(3) will become stronger (less antibonding).

Although the depopulation of the HOMO of the $Ru_3(CO)_8$ fragment appears to be the major factor which determines changes in the ruthenium triangle, other changes in metal fragment orbital populations must be considered. MOs 55, (Fig. 3), and 56 which were originally empty in the $Ru_3(CO)_8$ fragment, gain 0.33 and 0.10 electrons respectively. These changes lead to a minor strengthening of Ru(1)–Ru(2) and Ru(2)–Ru(3), and partially offset the loss of 1.1 electrons from MO 52.

Metal–metal vs. metal–acetylene bonding

The total Mulliken overlap populations for metal–acetylene bonding are large (0.111 to Ru(1), 0.214 to Ru(2), 0.111 to Ru(3)) and there is no doubt that the metal triangle experiences a "clamp" effect as the alkyne ligands bind to the metal framework. This we term "*indirect* metal–metal bonding". However, we have illustrated that metal triangle deformation can also be attributed to changed in *direct* metal–metal bonding. Obviously, the two effects are not mutually exclusive; depopulation of the HOMO of the $Ru_3(CO)_8$ fragment cannot occur in the absence of, for example, the acetylene ligands. However, we feel it is useful to point out that the triangle deformation is not simply a physical shrinking which is required in order to accommodate the alkyne ligands' "bite-size" [3].

Carbonyl ligand orientation

Figure 6 shows schematic representations of the structures of $Os_3(CO)_{12}$ and $Os_3(CO)_8(C_2Ph_2)_2$. Attention is drawn to the differences in carbonyl ligand orientation. The $Os_3(CO)_8$ fragment is generated from $Os_3(CO)_{12}$ by the removal of two axial carbonyl ligands from Os(2), and the removal of one carbonyl ligand from each of atoms Os(1) and Os(3). The positions of the three carbonyl ligands on Os(1) (and, by symmetry, Os(3)) in $Os_3(CO)_8(C_2Ph_2)_2$ can be derived from those of $Os_3(CO)_{12}$ either by removal of an axial or equatorial carbonyl ligand followed by deformation of the remaining ligands (Fig. 7). A change in the number of carbonyl ligands in going from $Os_3(CO)_{12}$ to $Os_3(CO)_8(C_2Ph_2)_2$ is clearly needed, as one can consider the transition as the double substitution of a 4-electron donor acetylene ligand for two carbonyls, each a 2-electron donor. An obvious explanation for the observed carbonyl rearrangement at atoms Os(1) and Os(3) is steric effects. A space filling diagram of $Os_3(CO)_8(C_2Ph_2)_2$ is given in Fig. 8. The close proximity of the phenyl groups to the carbonyl ligands shows that steric effects may indeed be important. However, by considering electronic factors, we illustrate below

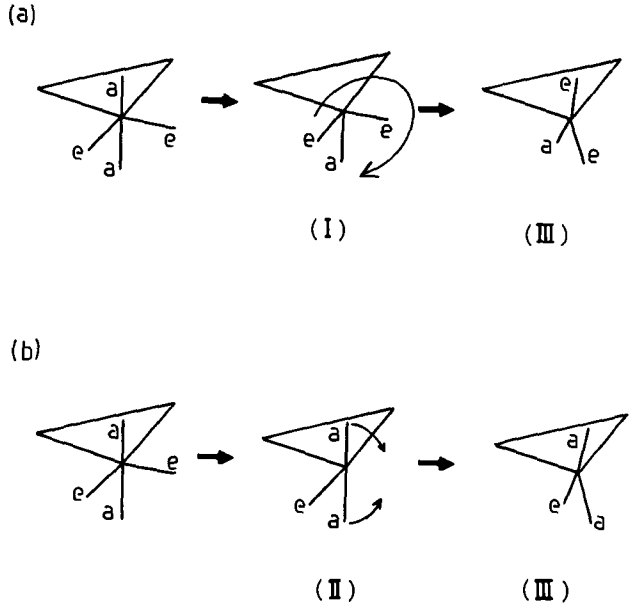

Fig. 7. Generation of the $M(CO)_3$ (M = Ru or Os) ligand arrangement at M(1) or M(3) in $M_3(CO)_8(C_2R_2)_2$ from $M_3(CO)_{12}$ (a) by removal of an axial ligand and (b) by removal of an equatorial ligand.

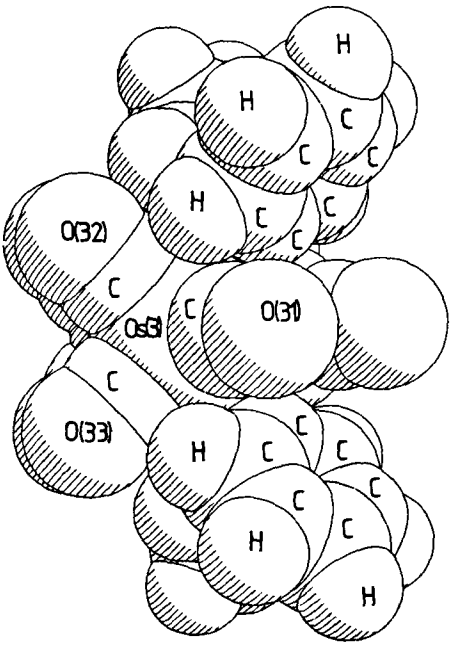

Fig. 8. Space filling diagram of $Os_3(CO)_8(C_2Ph_2)_2$.

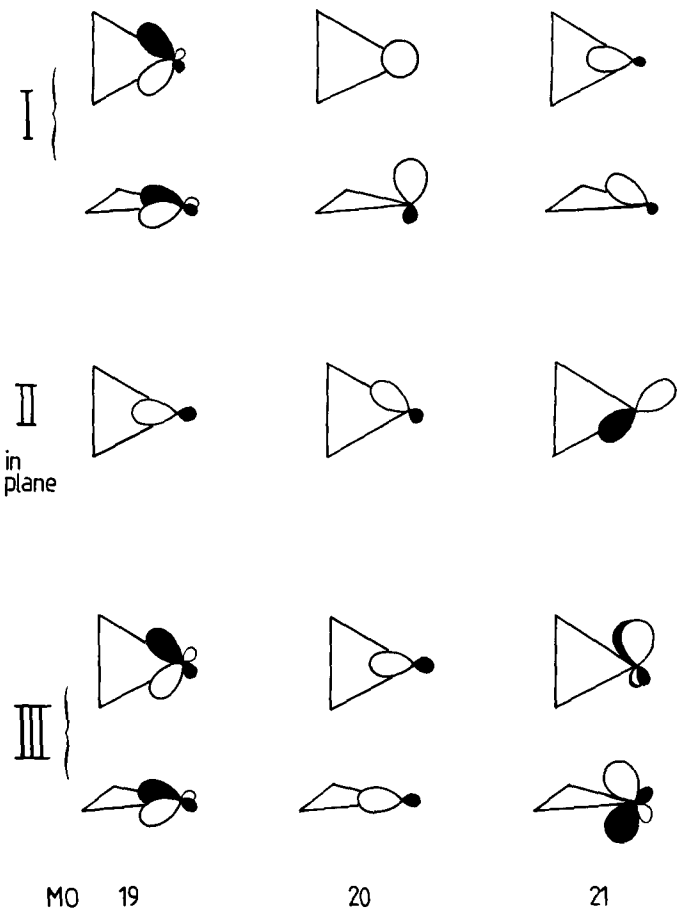

Fig. 9. Frontier molecular orbitals 19-21 of $Ru(CO)_3$ for structures I, II and III.

that reorientation of the carbonyl ligands is prerequisite to maximizing metal–acetylene bonding.

Beginning with the carbonyl ligands around Os(1) in $Os_3(CO)_{12}$, an axial ligand can be removed to generate the $Os(CO)_3$ unit shown in Fig. 7a, structure I. Alternatively, removal of an equatorial carbonyl ligand leads to structure II (Fig. 7b). The experimental geometry of the $Os(CO)_3$ unit, III, at Os(1) in $Os_3(CO)_8(C_2Ph_2)_2$ can be readily generated from either I or II (Fig. 7). By using $Ru_3(CO)_{12-x}(C_2H_2)_x$ to model $Os_3(CO)_{12-x}(C_2Ph_2)_x$, the frontier orbitals of the $Ru(CO)_3$ unit with structures I, II and III were compared. These MOs are schematically illustrated in Fig. 9. The frontier orbitals of the "conical" and "T-shaped" $Ru(CO)_3$ fragments have previously been described [13,14]. Since I and II are remnants of approximate octahedral arrangements of "ligands", (adjacent metal atoms included as well as carbonyls), one expects to see a frontier orbital pointing toward the vacant octahedral site [15,16]. This is indeed observed. The orbitals of the conical fragment, I, will only interact effectively with one of the alkyne ligands in $Ru_3(CO)_8(C_2H_2)_2$. Indeed, this carbonyl arrangement is observed in the mono-acetylene compound, $Os_3(CO)_{10}(C_2Ph_2)$ [17 *]. The T-shaped frag-

ment, II, possesses frontier orbitals which are in the plane of the metal triangle. The Ru(1) and Ru(3) fragments can, therefore, interact equally with the two C_2H_2 ligands. However, inter-fragment orbital interaction is increased significantly as the carbonyls are tipped back, i.e. in going from II to III. The most noticeable effect is that rehybridisation of MO 20 produces an out-of-plane orbital which points directly at the carbon atoms of the two alkynes. In addition, in II, MO 21 has less metal character than in III. Thus, we consider that the observed carbonyl arrangement in $Os_3(CO)_8(C_2Ph_2)_2$ is controlled, at least in part, by electronic effects, rather than wholly by steric effects.

Acknowledgements

We thank the S.E.R.C. for support (to S.M.O.) and Rajesh Khattar, Professor J. Lewis, Dr. B.F.G. Johnson, and Dr. P.R. Raithby for helpful discussions.

References

1 R.L. DeKock, P. Deshmukh, T.K. Dutta, T.P. Fehlner, C.E. Housecroft and J.L.-S. Hwang, Organometallics, 2 (1983) 1108.
2 B.E.R. Schilling and R. Hoffmann, J. Am. Chem. Soc., 101 (1979) 3456.
3 G. Granozzi, E. Tondello, M. Casarin, S. Aime and D. Osella, Organometallics, 2 (1983) 430.
4 R.L. DeKock, T.P. Fehlner, C.E. Housecroft, T. Lubben and K. Wade, Inorg. Chem., 21 (1982) 25.
5 S. Aime, R. Bertoncello, V. Busetti, G. Granozzi and D. Osella, Inorg. Chem., 25 (1986) 4004.
6 R.P. Dodge and V. Schomaker, J. Organomet. Chem., 3 (1965) 274.
7 B.F.G. Johnson, R. Khattar, L.J. Lahoz, J. Lewis, and P.R. Raithby, J. Organomet. Chem., 319 (1987) C51.
8 E.A. Seddon and K.R. Seddon, The Chemistry of Ruthenium, Monograph 19, Elsevier, 1984, p. 1051.
9 M.B. Hall and R.F. Fenske, Inorg. Chem., 11 (1972) 768.
10 E. Clementi, J. Chem. Phys. 40 (1964) 1944.
11 J.W. Richardson, M.J. Blackman and J.F. Ranochak, J. Chem. Phys., 58 (1973) 3010.
12 N.M. Kostić and R.F. Fenske, Inorg. Chem., 22 (1983) 666.
13 A. Stockis and R. Hoffmann, J. Amer. Chem. Soc., 102 (1980) 2952.
14 M. Elian and R. Hoffmann, Inorg. Chem., 14 (1975) 1058.
15 R. Hoffmann (Nobel Lecture) Angew. Chem., Int. Ed. Engl. 21 (1982) 711.
16 C.E. Housecroft and A.L. Rheingold, Organometallics, 6 (1987) 1332.
17 In going from $Os_3(CO)_{12}$ to $Os_3(CO)_{10}(C_2Ph_2)$, one axial CO ligand is removed from each of Os(1) and Os(2). An axial CO on Os(3) becomes semi-bridging along Os(1)–Os(3): C.G. Pierpont, Inorg. Chem., 16 (1977) 636.

* Reference number with asterisk indicates a note in the list of references.